We are IntechOpen, the world's leading publisher of Open Access books Built by scientists, for scientists

6,900
Open access books available

185,000
International authors and editors

200M
Downloads

Our authors are among the

154
Countries delivered to

TOP 1%
most cited scientists

12.2%
Contributors from top 500 universities



WEB OF SCIENCE™

Selection of our books indexed in the Book Citation Index in Web of Science™ Core Collection (BKCI)

Interested in publishing with us?
Contact book.department@intechopen.com

Numbers displayed above are based on latest data collected.
For more information visit www.intechopen.com



Chapter 13

A Treatise on Magnetic Surface Polaritons: Theoretical Background, Numerical Verification and Experimental Realization

Yu-Hang Yang and Ta-Jen Yen

Additional information is available at the end of the chapter

http://dx.doi.org/50752

1. Introduction

The polariton is a kind of coupling between electromagnetic waves (photons) and elementary excitations such as phonons, plasmons and magnons, It includes two modes of surface and bulk polariton that can be excited by means of semiconductors, metals, ferromagnets, antiferromagnets, and so on. The coupling causes an intensity enhancement of the electromagnetic field, which is very useful for nano-technology such as biosensing, waveguide applications, nano-antenna device. The majority of the literature is concentrating on the magnetic surface polariton supported by magnetic materials. The outline of paper is as follows. In sections 2 we introduce the fundamental of the polaritons first, and then the general dispersion equation of the magnetic surface polaritons (MSPs) mode by considering the full form of Maxwell's equations in section 3. Next, in sections 4 and 5, we present numerical and experimental results of realizing the MSPs, by naturally existing materials – in section 4, by ferromagnetic and antiferromagnetic materials and in section 5, by the effective media of ferromagnetic and anti-ferromagnetic superlattices, respectively. By employing metamaterials, artificially constructed materials whose properties mainly stem from structures rather than their constitutive elements, one can also achieve MSPs mode with a greater engineering freedom; thus, in section 6, we start from interpreting what metamaterials and their operation rationales are, and then how metamaterials support the MSPs mode. Finally, in section 7, there comes a conclusion. Note that in this study we moderately modify the quoted definitions in the diagrams to correspond to our definitions.

2. Fundamental of polaritons

The well-known surface plasmon polaritons (SPPs) denote that a collective oscillation of electrons couples with the transverse magnetic wave, and they propagate along the interface between two media (ex: a metal and a dielectric) with an exponential decay into two media. Due to the polarization dependence of SPPs, it is a reasonable perception to realize a magnetic

INTECH
open science | open minds

©2012 Yang and Yen, licensee InTech. This is an open access chapter distributed under the terms of the Creative Commons Attribution License (http://creativecommons.org/licenses/by/3.0), which permits unrestricted use, distribution, and reproduction in any medium, provided the original work is properly cited.

analog by a transverse electric wave. In addition, we have known the fact that the wave equation can be expressed by either electric or magnetic component of the electromagnetic wave, so that it implies that all electromagnetic phenomena chould be symmetric. In recent years, more and more researchers have paid intensive attention to the electric SPPs and their applications, in particular for bio-sensing [15] and nanophotonic applications [27].

In contrast, the magnetic surface polaritons (MSPs) mode did not attract much attention yet, and that is because magnetic responses are typically weak and their resonant frequencies are usually below the far infrared region. In our opinion, it is useful and interesting to understand the mechanism of the MSPs even it still does not yet become a protagonist. Throughout this study, we will show there is a potential material to promote the inherent magnetism in natural materials.

At first, let us briefly define the well-known magnetic polariton. In general, the magnetically ordered media support three kinds of elementary modes, spin waves (or call magnons), magnetostatic modes, and magnetic polaritons. Three modes are classified by the dominant restoring force as shown in Fig. 1 [21]. When the wavevector (k) in vacuum is greater than $10^8\ m^{-1}$, the exchange interaction is important and one calls this mode as magnon. The equation of motion is usually needed to solve this mode. For magnetostatic mode (magnetostatic limit, $k \ll \frac{\omega}{c}$), $10^7 \leqslant k \leqslant 10^8\ m^{-1}$, the exchange and dipolar interactions may be both important; $3 \times 10^3 \leqslant k \leqslant 10^7\ m^{-1}$, the dipolar terms are mainly dominant. For this region, we need a Hamiltonian treatment for such a magnetostatic mode. For magnetic polaritons, $k \leqslant 3 \times 10^3\ m^{-1}$, it is recognized as electromagnetic region where the full form of Maxwell's equations including retardation corrections have to be considered. As an example, the dispersion relation of a ferromagnetic insulator [21] is plotted in Fig. 1, in where ω_0 and ω_m will be defined later. In this literature, we just concentrate on MSPs, and study three situations: a pure ferromagnets (or antiferromagnets), ferromagnetic (or antiferromagnetic) superlattices, and magnetic metamaterials.

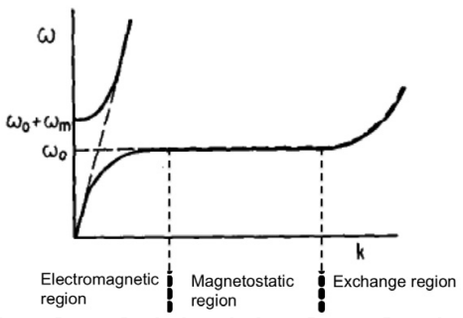


Figure 1. The dispersion diagram. In general, $k > 10^8\ m^{-1}$ is an exchange region; $3 \times 10^3 \leqslant k \leqslant 10^8\ m^{-1}$ is a magnetostatic region; $k \leqslant 3 \times 10^3\ m^{-1}$is an electromagnetic region.

3. General dispersion equation for magnetic surface polaritons

It is worthy to derive a general dispersion relation in advance before we begin studying the real cases. It should help one to understand all definitions that are used in our whole literature. First, the geometry considered in this study consists of two semi-infinite linear media, including the magnetic and nonmagnetic media shown in Fig. 2. Second, we assume

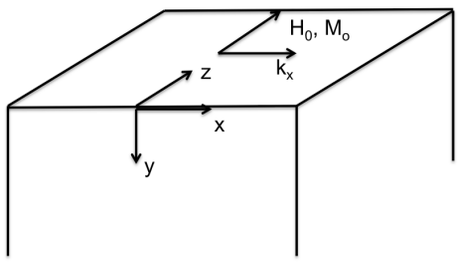


Figure 2. The geometry considered in this study. The half space above the $y > 0$ plane is a magnetic medium; below the $y < 0$ plane is a nonmagnetic medium. The external static magnetic field (H_0) is parallel to the easy axis, $\hat{z}$.

that the magnetic permeability tensor of the magnetic medium can be written by

$$\overleftrightarrow{\mu}_{eff}(\omega) = \begin{pmatrix} \mu_{xx} & i\mu_{xy} & 0 \\ -i\mu_{xy} & \mu_{yy} & 0 \\ 0 & 0 & \mu_{zz} \end{pmatrix}, \tag{1}$$

and the electric permittivity can be given by

$$\overleftrightarrow{\varepsilon}_{eff}(\omega) = \begin{pmatrix} \varepsilon_{xx} & 0 & 0 \\ 0 & \varepsilon_{yy} & 0 \\ 0 & 0 & \varepsilon_{zz} \end{pmatrix}. \tag{2}$$

Note that we are interesting in the dispersion relation itself so that the damping and spatial dispersion can be ignored here. It will be worthy to consider the damping only when the reflectivity calculation is executed; spatial dispersion is meaningful only for magnons. The constitutive relations for the linear medium read

$$\vec{D}(\omega) = \overleftrightarrow{\varepsilon}_{eff}(\omega)\vec{E}(\omega), \quad \vec{B}(\omega) = \overleftrightarrow{\mu}_{eff}(\omega)\vec{H}(\omega). \tag{3}$$

Next, we follow our previous work [37] and ready to derive rigorously a general dispersion equation. We are looking for MSPs mode. Therefore, without loss of generality, the transverse electric fields of the MSPs mode above and below the plane $y = 0$ can be respectively written by

$$\begin{aligned} \vec{E}^{+}(\omega) &= \hat{z}\,\mathrm{E}_z^{+} e^{ik_x x} e^{-\alpha^{+} y}, \\ \vec{E}^{-}(\omega) &= \hat{z}\,\mathrm{E}_z^{-} e^{ik_x x} e^{\alpha^{-} y}. \end{aligned} \tag{4}$$

where k_x is the direction of the MSPs mode in vacuum. α^{+} and α^{-} stand for attenuation coefficients of the MSPs mode for $y > 0$ and $y < 0$, respectively. Faraday's law can solve the corresponding magnetic induction as follows,

$$\begin{aligned} \vec{B}^{+}(\omega) &= \frac{1}{i\omega}\left[\left(-\alpha^{+}\right)\hat{x} - (ik_x)\,\hat{y}\right]\vec{E}^{+}(\omega), \\ \vec{B}^{-}(\omega) &= \frac{1}{i\omega}\left[\left(\alpha^{-}\right)\hat{x} - (ik_x)\,\hat{y}\right]\vec{E}^{-}(\omega). \end{aligned} \tag{5}$$

Next, the magnetic fields can be solved by Eq. 3:

$$\begin{aligned} \vec{H}^{+}(\omega) &= \frac{-1}{\mu_{xy}^2 - \mu_{xx}\mu_{yy}}\left[\left(-\mu_{yy}\alpha^{+} + \mu_{xy}k_x\right)\hat{x} + \left(-i\mu_{xy}\alpha^{+} - i\mu_{xx}k_x\right)\hat{y}\right], \\ \vec{H}^{-}(\omega) &= \left(-\alpha^{+}\right)\hat{x} + (-ik_x)\,\hat{y}. \end{aligned} \tag{6}$$

Applying Ampere's law with Eqs. 1-3, we can solve the following wave equations:

$$\begin{aligned}&\left[\mu_{xx}\frac{\partial^2}{\partial x^2}+\mu_{yy}\frac{\partial^2}{\partial y^2}+\left(\mu_{xx}\mu_{yy}-\mu_{xy}^2\right)\frac{\omega^2}{c^2}\varepsilon_{zz}\right]\vec{E}^{+}(\omega)=0,\\&\left(\frac{\partial^2}{\partial x^2}+\frac{\partial^2}{\partial y^2}+\frac{\omega^2}{c^2}\varepsilon_{zz}\right)\vec{E}^{-}(\omega)=0.\end{aligned}\tag{7}$$

Using Eqs. 4 and 7, we can solve the attenuation coefficients as follows,

$$\begin{aligned}\alpha^{+}&=\sqrt{\frac{\mu_{xx}}{\mu_{yy}}k_x^2-\left(\frac{\mu_{xx}\mu_{yy}-\mu_{xy}^2}{\mu_{yy}}\right)\frac{\omega^2}{c^2}\varepsilon_{zz}},\\\alpha^{-}&=\sqrt{k_x^2-\frac{\omega^2}{c^2}}.\end{aligned}\tag{8}$$

Note that it is also straightforward to solve the bulk polaritons, propagating perpendicular to the $\hat{z}$ axis. All we do is just to replace $\alpha^{\pm}$ by ik_y. Then, one is given by

$$\begin{aligned}\frac{c^2\left(\mu_{xx}k_x^2+\mu_{yy}k_y^2\right)}{\omega^2}&=\left(\mu_{xx}\mu_{yy}-\mu_{xy}^2\right)\varepsilon_{zz},\\k_x^2+k_y^2&=\frac{\omega^2}{c^2}.\end{aligned}\tag{9}$$

The continuity of the tangential components of the electric field (E_x) and the magnetic filed (H_x) at the interface ($y=0$) yields

$$E_x^{+}=E_x^{-},\ \ \frac{\mu_{yy}B_x^{+}+i\mu_{xy}B_y^{+}}{\mu_{xx}\mu_{yy}-\mu_{xy}^2}=\alpha^{-}.\tag{10}$$

Using the Eqs. 5, 6 and 10, the general dispersion equation of the MSP's mode reads

$$\frac{-\alpha^{+}\mu_{yy}+\mu_{xy}k_x}{\mu_{xx}\mu_{yy}-\mu_{xy}^2}=\alpha^{-}.\tag{11}$$

Note that Eq. 11 itself implies a non-reciprocal dispersion relation due to $\pm|k_x|$. Now, we have enough equations to begin our discussion for the MSPs mode.

4. Realization of MSPs mode by magnetic materials

Over the past 50 years, Damon and Eshbach [8] first reported the surface magnetostatic modes without retardation effect for the case of a ferromagnetic slab; effective media for superlattices have also done [17]. Later Hartstein et al. reported more detailed discussion of the MSPs for semi-infinite medium of a pure magnetic materials [1]. Before discussing the semi-infinite gyromagnetic uniaxial medium (gyromagnetic ratio,$\gamma \neq 0$), we have to assume several limitations for this study: (a) we neglect the local effects of the surface on the spin wave (i.e. pinning effects) and (b) the exchange interaction is ignored as well.

4.1. Semi-infinite ferromagnets

In this part, we consider the case, a pure ferromagnet and vacuum. For simplicity, we treat the electric permittivity of a ferrromagnet [$\overleftrightarrow{\varepsilon}(\omega)$] as scalar value, 1. Also, we neglect damping of $\overleftrightarrow{\mu}(\omega)$ so that μ_{xx}, μ_{zz}, and μ_{xy} in Eq. 1 are real. The external static magnetic filed (H_0) is along the easy axis $+\hat{z}$ shown in Fig. 2. The half space $y < 0$ is vacuum, and $y > 0$ is a pure ferromagnet. In the Voigt geometry, the magnetic permeability satisfies the equation, $\mu_v(\omega) = \mu_{xx} - \mu_{xy}^2 \big/ \mu_{xx}$ plotted in Fig. 3 [1]. We also define $\omega_v = \gamma\sqrt{B_o H_0}$ at resonance and $\omega_1 = \gamma B_0$ at $\mu_v(\omega) = 0$. For a uniaxial ferromagnet ($\mu_{xx} = \mu_{yy}$), the Eqs. 8 and 11 are rewritten by

$$\alpha^+ = \sqrt{k_x^2 - \mu_v \frac{\omega^2}{c^2}}, \quad \alpha^- = \sqrt{k_x^2 - \frac{\omega^2}{c^2}}. \tag{12}$$

and

$$\frac{-\alpha^+ \mu_{xx} + \mu_{xy} k_x}{\mu_{xx}^2 - \mu_{xy}^2} = \alpha^-. \tag{13}$$

For the MSPs mode, the α^+ and α^- in Eq. 12 have to be positive that yield to an exponential

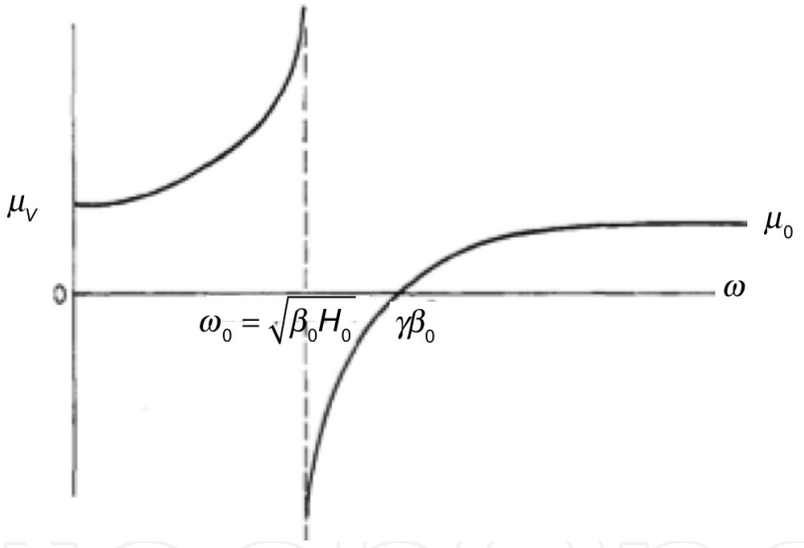


Figure 3. Frequency dependence of magnetic permeability in the Voigt geometry. [1]

decay into both magnetic and nonmagnetic materials (vacuum). The dispersion diagram [1] is plotted in Fig. 4 in where the shaded region makes the existence of the MSPs mode possible. For a uniaxial ferromagnet, the components of the magnetic permeability tensor in Eq. 1 can be written by

$$\begin{aligned} \mu_{xx} &= \mu_{yy} = \mu_0 \left(1 + \frac{\omega_m \omega_0}{\omega_0^2 - \omega^2}\right), \\ \mu_{zz} &= \mu_0, \\ \mu_{xy} &= \mu_0 \frac{\omega_m \omega}{\omega_0^2 - \omega^2}. \end{aligned} \tag{14}$$

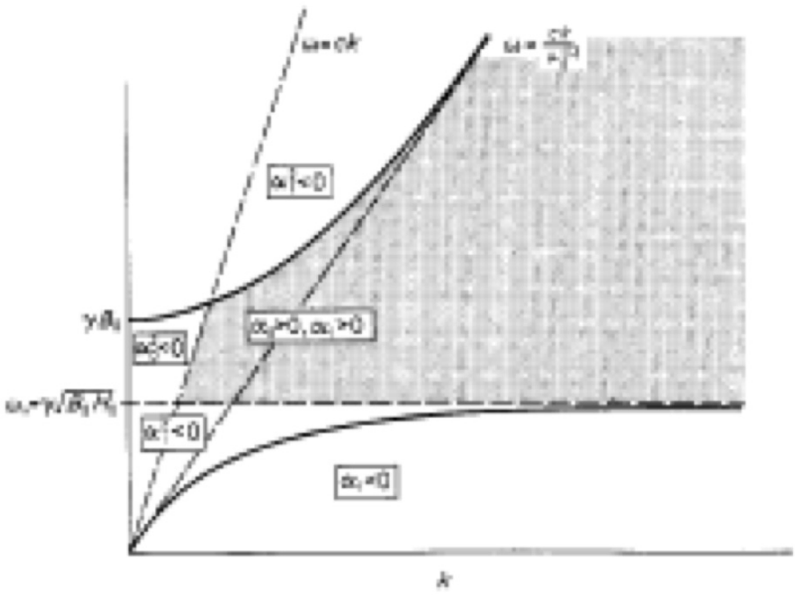


Figure 4. The dispersion relation of a pure ferromagnet. [1]

Here, two angular frequencies (ω_m and ω_0) are written in terms of the magnetization (M_0) and external field (H_0):

$$\omega_m = 4\pi\gamma M_0, \;\; \omega_0 = \gamma H_0, \tag{15}$$

where ω_0 is angular frequency of the ferromagnetic resonance, and γ is the gyromagnetic ratio. Note that μ_0 in Eq. 14 is caused by other magnetic dipole excitation (such as optical magnons) at higher frequency (ex: $\mu_0 = 1.25$ in YIG). Before discussing a detailed calculation of dispersion equation, we would like to return to Eq. 6 that can simply predict a non-reciprocal dispersion relation. One write down the polarization of the magnetic field of the MSPs at a fixed point by investigating the components in Eq. 6:

$$\frac{H_y^+}{H_x^+} = i\frac{\mu_{xy}\alpha^+ + \mu_{xx}k_x}{\mu_{yy}\alpha^+ - \mu_{xy}k_x}. \tag{16}$$

When we take the magnetostatic limits ($k_x \to \pm\infty$), $\alpha^{\pm}$ will be very close to $|k_x|$ [see Eq. 12]. Then, the Eq. 16 reduces to $H_y^+ = iH_x^+$ for the $+k_x$ direction and $H_y^+ = -iH_x^+$ for the $-k_x$. Therefore, the polarization of magnetic field of the MSPs mode has a different rotation for different $\pm k_x$ directions, leading to a non-reciprocal result. Next, we are ready to investigate it in detail by solving the Eq. 13 at the magnetostatic limit $k_x \to \pm\infty$. One is given by

$$\mu_{xx} \pm \mu_{xy} \equiv \mu_{\rho\pm}(\omega) = -1. \tag{17}$$

Using Eq. 14, we write

$$\mu_{\rho\pm} = \mu_0\left(1 + \frac{\omega_m}{\omega_0 \mp \omega}\right) = -1. \tag{18}$$

Eq. 18 describes a condition to which the MSPs mode have a magnetostatic analog. Plotting a dispersion relation of the surface polariton [Eq. 13] is a good method to observe the condition shown in Fig. 5. Note that an applied static field is already considered in Fig. 5. It is very clear to observe the non-reciprocal nature of the MSPs mode (solid curves). Next, we consider

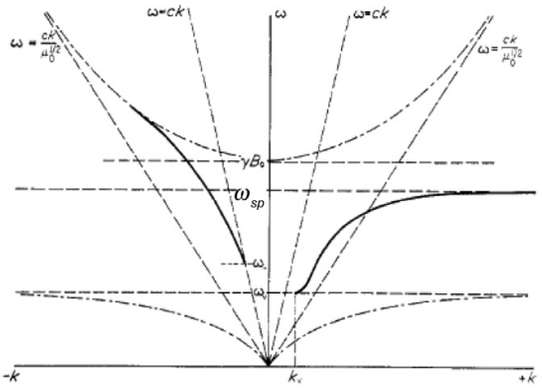


Figure 5. Non-reciprocal relation. The solid curves are the surface polaritons, and dot-dash curves are bulk polaritons. [1].

four situations: (a) For the magnetostatic limit $k_x \to +\infty$, we take $\mu_{\rho+}$ in Eq. 18, and then the frequency of the asymptotic surface polaritons reads

$$\omega_{sp} = \gamma \left(\frac{H_0 + \mu_0 B_0}{1 + \mu_0} \right), \tag{19}$$

where $B_0 \equiv H_0 + 4\pi\gamma M_0$. This is just the frequency of the unretardated surface magnon mode (also termed as DE mode [8]). (b) For the magnetostatic limit $k_x \to -\infty$, we find that $\mu_{\rho-}$ is always positive, yielding to no magnetostatic angalog. In general, the MSPs mode is called as real mode if magnetostatic limit is valid; otherwise, it is a virtual mode. Therefore, a non-reciprocal nature of the MSPs mode in a pure ferromagnet is acknowledged according to a magnetostatic mode. The investigation is in a good agreement with abovementioned polarization of magnetic field. (c) Next, let us consider a special case, $\mu_0 = 1$, and for the moment we concentrate on the $+k_x$ solution. The frequency of the MSPs mode starts at

$$\omega_v = \gamma \sqrt{B_0 H_0}, \tag{20}$$

and from Eq. 13 one obtains a corresponding wavevector

$$k_v = \frac{\omega_v}{c} \sqrt{\frac{B_0}{B_0 - H_0}} > \frac{\omega_v}{c}, \tag{21}$$

where the retardation corrections are already involved. The ω_v is also the frequency for the bulk magnon excitation under a condition, $\mu_v(\omega) \to \pm\infty$ [see Fig. 3]. If there is no external field, the ω_v reduces to zero so that the dispersion relation of the MSPs mode begins from the zero wavevector. The situation just likes electric SPPs supported by a dielectric and a metal [24]. (d) Now, let us consider the $-k_x$ solution including the retardation corrections. The retarded MSPs mode begins at the light line where $\mu_{xx}(\omega_-) = 1$ [see Fig. 5]. We solve Eq. 14 to yield the beginning frequency:

$$\omega_- = \gamma \sqrt{\frac{H_0^2 + \mu_0 H_0 B_0}{\mu_0 - 1}}. \tag{22}$$

Such a virtual mode terminates on the upper branch of the bulk polaritons. In addition, we see that from Eq. 22 the MSPs mode never starts at $\mu_0 \to 1$ (i.e. $\omega_- \to \infty$). Compared

Fig. 3 with Fig. 5, we note that the MSPs mode in the $-k_x$ direction still can exist even if $\mu_v > 1$. It is a very different from isotropic medium ($\mu_{xx} = \mu_{yy} = \mu_{zz}$) because its MSPs mode is only found within a gap where $\mu_v < 1$. From Eq. 21, the light line cannot excite any MSPs mode due to lack of the momentum conservation. In order to excite the MSPs mode in a pure ferromagnet, the optical coupler is need to transfer the momentum of the light to MSPs mode. Here, we quote the reference [[14]] to show the numerical calculations of the reflectivity spectra of the MSPs mode. Note that the damping factor is no longer neglected when one calculates a reflectivity spectrum. In Fig. 6, the calculated reflectivity spectra result from Otto ATR [1] configuration (optical coupler) for a pure ferromagnet (YIG). The figures 6(a) and 6(b) correspond to $+k_x$ and $-k_x$ directions, respectively. "h" is the air gap between a prism and a YIG. In Fig. 6(a), it shows that a larger damping ($1/\tau$) of the MSPs has larger loss, leading to much difficulty for determining the resonance frequency. In Fig. 6(b), the resonance frequency of the MSPs mode is blue-shift among increasing incidence angles. The asymmetric reflectivity deep results from an appreciable photon content in both figures 6. In general, the resonance frequency of the MSPs mode for a pure ferromagnet lies in a microwave region so that one needs a big sample for measuring the MSPs mode. There is, as we know, not a direct experimental verification.

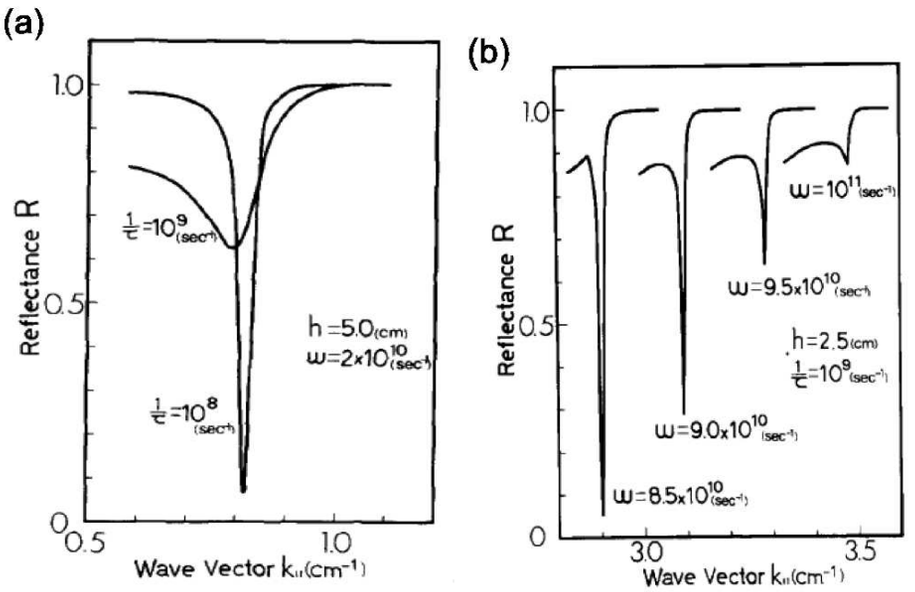


Figure 6. (a) The Otto ATR spectra at the $+k_x$ for different time relaxation (τ). (b) The ATR at the $-k_x$ for different incidence angle within the prism. [14]

4.2. Semi-infinite antiferromagnets

In this case, we focus on a gyromagnetic uniaxial antiferromagnetic medium in the Voigt configuration. Again, we neglect the exchange interactions and damping of $\overleftrightarrow{\varepsilon}(\omega)$ and $\overleftrightarrow{\mu}(\omega)$, and the external static magnetic field is applied in the $\hat{z}$ direction. The magnetization (M_0) splits the ferromagnetic resonant frequency (ω_0) into two separable frequencies given as $\omega_\pm = \omega \pm \omega_0$. The effective magnetic permeability can be derived by considering Bloch's

[1] attenuated total reflectance

equations [20], which reads

$$\begin{aligned}
\mu_{xx} &= \mu_{yy} = \mu_0 \left(1 + \frac{\omega_m \omega_A}{\omega_{an}^2 - \omega_+^2} + \frac{\omega_m \omega_A}{\omega_{an}^2 - \omega_-^2}\right), \\
\mu_{zz} &= \mu_0, \\
\mu_{xy} &= \mu_0 \left(\frac{\omega_m \omega_A}{\omega_{an}^2 - \omega_+^2} - \frac{\omega_m \omega_A}{\omega_{an}^2 - \omega_-^2}\right),
\end{aligned} \tag{23}$$

where ω_{an} is the antiferromagnetic resonance frequency and is determined by the anisotropy field (H_A) and exchange field (H_E),

$$\omega_{an} = \sqrt{\omega_A \left(2\omega_E + \omega_A\right)} = \gamma \sqrt{H_A \left(2H_E + H_A\right)}, \tag{24}$$

where $\omega_A = \gamma H_A$ and $\omega_E = \gamma H_E$. Next, one just follows the Eq. 8, yielding to Eq. 25,

$$\begin{aligned}
\alpha^+ &= \sqrt{k_x^2 - \left(\frac{\mu_{xx}^2 - \mu_{xy}^2}{\mu_{xx}}\right) \frac{\omega^2}{c^2} \varepsilon_{zz}}, \\
\alpha^- &= \sqrt{k_x^2 - \frac{\omega^2}{c^2}}.
\end{aligned} \tag{25}$$

Also, the dispersion relation from Eq. 11 can read

$$\frac{-\alpha^+ \mu_{xx} + \mu_{xy} k_x}{\mu_{xx}^2 - \mu_{xy}^2} = \alpha^-. \tag{26}$$

In the absence of the applied field ($H_0 = 0$), one has $\mu_{xy} = 0$ [see Eqs. 15 and 23]. Then, Eqs. 25 and 26 reduce more compact forms:

$$\begin{aligned}
\alpha^+ &= \sqrt{k_x^2 - \varepsilon_{zz} \mu_{xx} \frac{\omega^2}{c^2}}, \\
\alpha^- &= \sqrt{k_x^2 - \frac{\omega^2}{c^2}}.
\end{aligned} \tag{27}$$

$$\frac{-\alpha^+}{\mu_{xx}} = \alpha^-. \tag{28}$$

Using Eqs. 27 and 28 together, a simpler dispersion relation of surface polariton can be given by

$$k_x^2 \left(1 - \mu_{xx}^2\right) = \frac{\omega^2}{c^2} \mu_{xx} \left(\varepsilon_{zz} - \mu_{xx}\right). \tag{29}$$

The simpler dispersion relation [5] is plotted in Fig. 7. In Fig. 7, we can observe the reciprocal property of the MSPs mode. Also, it is straightforward to calculate the frequency of the

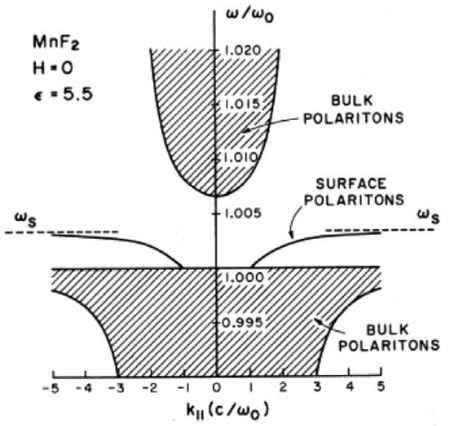


Figure 7. The shaped areas are bulk polaritons, and two solid curves are surface polaritons. Without an external static magnetic field, the dispersion relation is reciprocal. ($H_0 = 0$, $\varepsilon_{zz} = 5.5$) [5]

MSPs mode at the magnetostatic limit. One just solves $\mu_{xx} = -1$ [see Eq. 28] and yields the asymptotic frequency of MSPs shown in Fig. 7 as follows,

$$\omega_s = \sqrt{\omega_{an}^2 + \omega_m \omega_A}. \tag{30}$$

On other hand, with an applied static field, Eq. 26 has to be solved numerically shown in Fig. 8 [5]. Interestingly, one can clearly see the non-reciprocal dispersion relation of the MSPs mode that is just like a pure ferromagnet case with an applied static field. Note that the third MSPs mode starts at near $\omega/\omega_0 = 1.01$ and has no magnetostatic analog (i.e. virtual mode). However, two MSPs modes at lower frequency region have magnetostatic limits (i.e. ω_{sm+} and ω_{sm-}).

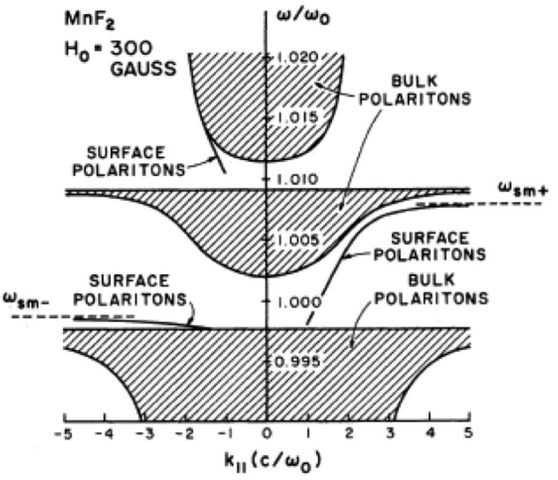


Figure 8. Dispersion relation for MSPs mode on MnF_2 at an applied field of 300 G. There are two real modes and virtual mode that are all non-reciprocal modes. [5]

Now, we would like to talk about the experimental verification for the surface polaritons. Let's simply describe the numerical results. There are typically two kinds of couplers: ATR and diffraction gratings. Here, we quote reference [32] in where they considered the diffraction gratings. In Fig. 9, the sample is MnF_2, a uniaxial antiferromagnet with the parameters $H_E = 7.87\ KG$, $H_A = 550\ HG$, $M_0 = 0.6\ KG$, and $\varepsilon_{zz} = 5.5$. Here, the Ω is our previous definition of antiferromagnetic resonance frequency, ω_{an}. There two solid lines are light lines ($k_x = \omega_0/c$),

and two dotted vertical lines correspond to the wavevectors induced by the gratings ($q = k_x \pm s$). It is clear to observe that light lines never interact any of the branch of MSPs mode (dash curves). However, wavevector induced by gratings ($q = k_x + s$) indeed interacts a MSPs mode at the direction ($+k_x$), leading to the excitation of the MSPs mode. Note that when Eq. 1 includes damping terms, the leaky MSPs modes appear as shown by solid curves in Fig. 9. The difficulty to observe the surface polaritons for a pure antiferromagnet should be easier than a pure ferromagnet. The reason is that the resonance frequency of the MSPs mode lies at far infrared regions and the sample need not be so large. M.R.F. Jensen et al reported the first direct experimental evidence [18] for a pure antiferromagnet (FeF_2, $\omega_{an} \sim 1.57\ THz$).

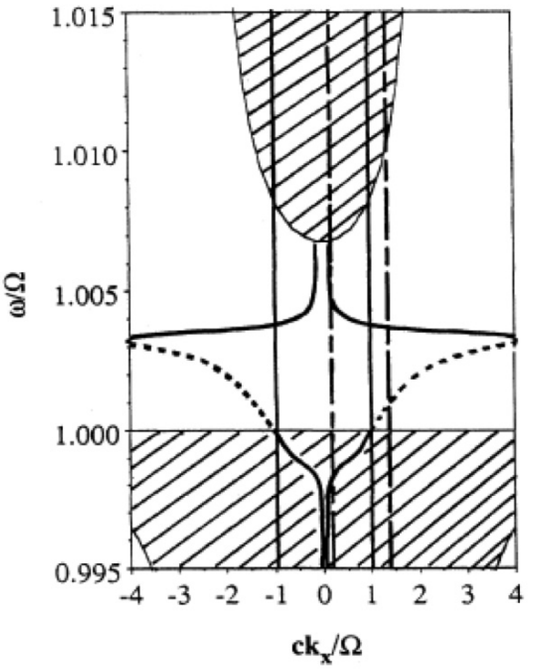


Figure 9. The shaped areas are bulk modes and the dashed lines are surface modes at no applied static field. The dotted vertical lines are the grating induced lines ($q = k_x \pm s$), and the light line is solid line ($q = k_x \pm s$). "s" is a reciprocal spatial period of the gratings. [[32]]

5. Realization of MSPs by effective media of magnetic superlattices

There are many researches on superlattice's surface polariton such as lateral superlattices [23, 36]. However, the lateral superlattice cases will be excluded in this study. In this section, the period of the superlattices will only to be along $\widehat{y}$ axis. The superlattices considered here is composed of two alternating uniaxial magnetic materials and uniaxial magnetic (or nonmagnetic) materials ($\mu_{xx}^{(j)} = \mu_{yy}^{(j)}$, $j =$ medium 1 or 2). Proposed that the condition, $kd << 1$ (period, $d = a + b$, see Fig. 10) is valid, and then the effective medium theory can adequately approximate the bulk and surface polaritons.

The magnetic permeability of each layer in a magnetic superlattices still can be respectively described by Eq. 1, and then we quote references [2, 25] that rigorously derived the effective magnetic permeability and electric permittivity of the magnetic superlattices. Therefore, one

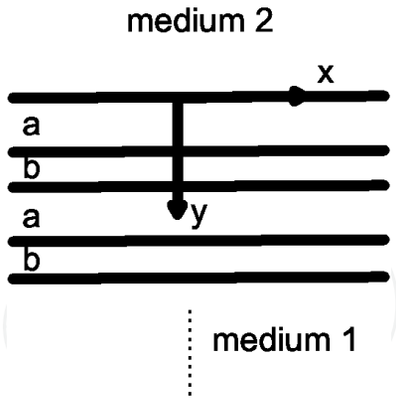


Figure 10. The region $y > 0$ is the magnetic superlattices composed of two alternating materials. The symbol "a" stands for the thickness of a ferromagnetic (or antiferromagnetic) material; "b" stands for the thickness of a nonmagnetic materials. $d = a + b$ is a period of two alternating magnetic materials.

is given by

$$\begin{aligned}
\bar{\mu}_{xx} &= \frac{(a+b)^2 \mu_{xx}^{(1)} \mu_{xx}^{(2)} + ab\left[\left(\mu_{xx}^{(1)} - \mu_{xx}^{(2)}\right)^2 - \left(\mu_{xy}^{(1)} - \mu_{xy}^{(2)}\right)^2\right]}{(a+b)\left(a\mu_{xx}^{(2)} + b\mu_{xx}^{(1)}\right)}, \\
\bar{\mu}_{yy} &= \frac{(a+b)\,\mu_{xx}^{(1)} \mu_{xx}^{(2)}}{a\mu_{xx}^{(2)} + b\mu_{xx}^{(1)}}, \\
\bar{\mu}_{xy} &= \frac{a\mu_{xy}^{(1)} \mu_{xx}^{(2)} + b\mu_{xy}^{(2)} \mu_{xx}^{(1)}}{a\mu_{xx}^{(2)} + b\mu_{xx}^{(1)}}, \\
\bar{\varepsilon}_{zz} &= \frac{a\varepsilon_{zz}^{(1)} + b\varepsilon_{zz}^{(2)}}{a+b}.
\end{aligned} \tag{31}$$

Most works on magnetic superlattices have almost considered the special case, that is, medium 2 is nonmagnetic ($\mu_{xx}^{(2)} = 1$ and $\mu_{xy}^{(2)} = 0$). Here, we also concentrate on such special case. Accordingly, we substitute Eq. 14 into $\mu_{xx}^{(1)}$ and $\mu_{xy}^{(1)}$ in Eq. 31 for ferromagnetic/nonmagnetic superlattices; for antiferromagnetic/nonmagnetic superlattices, Eq. 23 may be chosen. For both cases, an external static magnetic filed (H_0) is applied along the easy axis $+\hat{z}$.

5.1. Ferromagnetic superlattices

In the ferromagnetic superlattices case, we see $\bar{\mu}_{xx} \neq \bar{\mu}_{yy}$ and $\bar{\mu}_{xy} = a\mu_{xy}^{(1)} \Big/ \left(a + b\mu_{xx}^{(1)}\right)$ so that the attenuation coefficients and dispersion equation of the MSPs mode can be given by [see Eqs. 8 and 11]

$$\begin{aligned}
\alpha^+ &= \sqrt{\frac{\bar{\mu}_{xx}}{\bar{\mu}_{yy}} k_x^2 - \left(\frac{\bar{\mu}_{xx}\bar{\mu}_{yy} - \bar{\mu}_{xy}^2}{\bar{\mu}_{yy}}\right)\frac{\omega^2}{c^2}\bar{\varepsilon}_{zz}}, \\
\alpha^- &= \sqrt{k_x^2 - \frac{\omega^2}{c^2}},
\end{aligned} \tag{32}$$

and

$$\frac{-\alpha^{+}\bar{\mu}_{yy}+\bar{\mu}_{xy}k_x}{\bar{\mu}_{xx}\bar{\mu}_{yy}-\bar{\mu}_{xy}^2}=\alpha^{-}. \tag{33}$$

Again, Eq. 33 directly depends on the direction of k_x, leading to non-reciprocal dispersion relation. We would like to quote the results of the reference [4], and then the dispersion relation (Eq. 33) is rewritten as follows,

$$\left(\alpha^{-}\right)^2\bar{\mu}_{xx}\bar{\mu}_v-2\left(\alpha^{-}\right)\bar{\mu}_{xx}\bar{\mu}_v-k_x^2+\bar{\mu}_{xx}\frac{\omega^2}{c^2}=0. \tag{34}$$

where we substitute α^{+} in Eq. 32. The numerical calculation of Eq. 34 is shown in Fig. 11 at the condition, $a=b$. Note that we re-define the expression in the Eq. 15 for the reason to be consistent with reference [4]:

$$\omega_0=g\mu_0\gamma_0H_0,\ \ \omega_m=g\mu_0\gamma_0M_0, \tag{35}$$

where g is a Lande factor, μ_0 is a magnetic permeability in the vacuum, and $\gamma_0=e/2m$ with $e>0$ and m being the electron charge and electron mass. The numerical results show no magnetostatic analog (real mode) for this configuration (i.e. $a=b$) at $k_x\to\pm\infty$, and only a virtual mode exists for $-k_x$. For $a>b$, the magnetostatic analog can occurs at $-k_x$ (the evidence is not shown here). In addition, if the retardation corrections are included, then the virtual MSPs mode still exists for $a<b$. Note that Fig. 11 shows that the surface polaritons exist only in a restricted range.

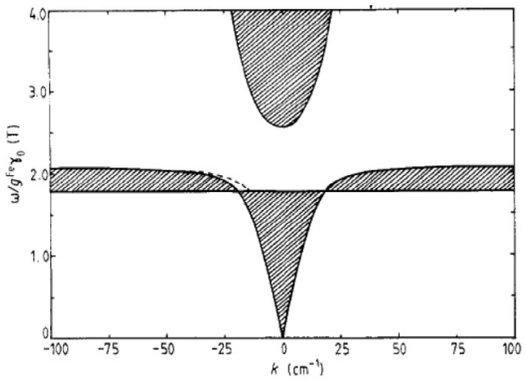


Figure 11. Ferromagnetic (Fe)/nonmagnetic superlattices. $a=b=5\times10^{-4}\ cm$. $\mu_0H_0=1\ T$. $\mu_0M_0=2.15\ T$. $g^{Fe}=2.15$. The shaped region is the bulk mode; the dotted line is the surface mode. [4]

5.2. Antiferromagnetic superlattices

Let us consider the superlattices that are composed of medium 1 (uniaxial antiferromagnetic) alternating with medium 2 (non-magnetic). In the absence of an applied static magnetic field ($H_0=0$), the component of the magnetic permeability of two media can read from Eq. 23,

$$\begin{aligned}
&\mu_{xx}^{(1)}=\mu_{yy}^{(1)}=1+\frac{2\omega_m\omega_A}{\omega_{an}^2-\omega^2}=\frac{\omega_1^2-\omega^2}{\omega_{an}^2-\omega^2}\equiv\mu_1,\\
&\mu_{xx}^{(2)}=\mu_{yy}^{(2)}=1\equiv\mu_2,\\
&\mu_{zz}^{(1)}=\mu_{zz}^{(2)}=\mu_0=1,\\
&\mu_{xy}^{(1)}=\mu_{xy}^{(2)}=0.
\end{aligned} \tag{36}$$

where $\omega_1 = \sqrt{\omega_{an}^2 + 2\omega_m\omega_A}$ at $\mu_1 = 0$. Here, we do not attempt to derive the non-reciprocal dispersion equation at an applied static field, but just show the numerical results later. Using Eqs. 31 and 36, the component of the effective magnetic permeability can be given by

$$\begin{aligned} \bar{\mu}_{xx} &= \frac{\bar{\omega}_1^2 - \omega^2}{\omega_{an}^2 - \omega^2}, \\ \bar{\mu}_{yy} &= \frac{\omega_1^2 - \omega^2}{\bar{\omega}_{an}^2 - \omega^2}, \end{aligned} \tag{37}$$

where $\bar{\omega}_1^2 = \left(b\omega_{an}^2 + a\omega_1^2\right)/(a+b)$ and $\bar{\omega}_{an}^2 = \left(a\omega_{an}^2 + b\omega_1^2\right)/(a+b)$. Reference [3] showed the results of Eq. 37 in Fig. 12 for $a > b$.

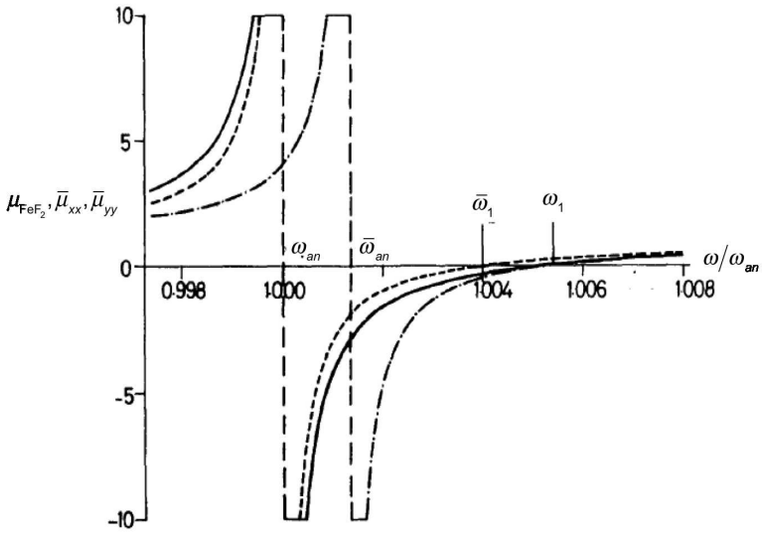


Figure 12. A FeF_2/ZnF_2 superlattices with $\frac{a}{a+b} = 0.75$. μ_{FeF_2} (solid line), $\bar{\mu}_{xx}$ (dash line), and $\bar{\mu}yy$ (dash-dot line). ω_{an}, $\bar{\omega}_{an}$, $\bar{\omega}_1$ and $\bar{\omega}_1$ are marked. [3]

Now the attenuation coefficients can be given by Eq. 8

$$\begin{aligned} \alpha^+ &= \sqrt{\frac{\bar{\mu}_{xx}}{\bar{\mu}_{yy}}k_x^2 - \bar{\varepsilon}_{zz} \cdot \bar{\mu}_{xx}\frac{\omega^2}{c^2}}, \\ \alpha^- &= \sqrt{k_x^2 - \frac{\omega^2}{c^2}}. \end{aligned} \tag{38}$$

And, the general dispersion equation of the MSPs mode reads from Eq. 11

$$\frac{-\alpha^+}{\bar{\mu}_{xx}} = \alpha^-, \tag{39}$$

Note that Eq. 39 implies a reciprocal dispersion relation of the surface polaritons. Substitution of Eq. 38 into Eq. 39 can solve the explicit form

$$k_x = \frac{\omega}{c}\sqrt{\frac{\bar{\mu}_{yy}\left(\bar{\mu}_{xx} - \bar{\varepsilon}_{zz}\right)}{\bar{\mu}_{xx}\bar{\mu}_{yy} - 1}}. \tag{40}$$

Eqs. 39 and 40 describes the condition for the existence of the MSPs mode. First, we investigate the magnetostatic limit ($k_x \to \pm\infty$), yielding to

$$\bar{\mu}_{xx} = -1,\ \bar{\mu}_{xx}\bar{\mu}_{yy} = 1. \tag{41}$$

We define $\bar{\mu}_{yy} < 0$ as real mode and $\bar{\mu}_{yy} > 0$ as virtual mode. In a result, only the real mode has a magnetostatic analog, and the virtual mode does not. Here, we simply persent two kinds of situations: (1) If $a > b$, the real mode lies in a frequency region, $\bar{\omega}_{an} < \omega < \omega_{sp}$ (i.e. $\bar{\mu}_{yy} < 0$) and virtual mode in another frequency region, $\omega_{an} < \omega < \bar{\omega}_{an}$ (i.e. $\bar{\mu}_{yy} > 0$) [see Fig. 12]. At $k_x \to \pm\infty$, Eq. 41 yields the asymptotic frequency of the MSPs mode

$$\omega_{sp} = \sqrt{\frac{\omega_{an}^2 + \omega_1^2}{2}}, \tag{42}$$

where $\omega_1 = \sqrt{\omega_{an}^2 + 2\omega_m\omega_A}$ at $\mu_1 = 0$ [see Eq. 36]. Note that the resonance frequency of the MSPs mode is independent of a and b and, consequently, is just the same as a pure antiferromagnet (see Eq. 30). (2) For $a < b$, there is only the virtual mode to exist at the frequencies, $\omega_{an} < \omega < \bar{\omega}_1$.

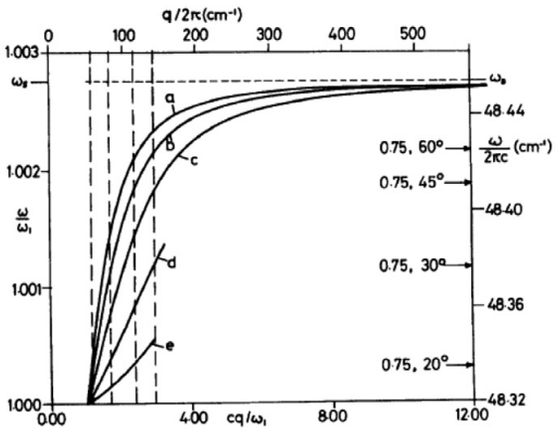


Figure 13. The dispersion relation versus f_1 at no applied static magnetic field ($H_0 = 0$). The curves from a to e represent $f_1 = 1,\ 0.75,\ 0.5,\ 0.25,$ and 0.1, respectively. [3]

For the FeF_2/ZnF_2 system, reference [3] has summarized the results of the dispersion curves of the MSPs modes versus $f_1 \equiv a/(a+b)$ various at $+k_x$ shown in Fig. 13. Figure 13 marks four black arrows for $f_1 = 0.75$ that respectively corresponds to four incidence angle: 20°, 30°, 45°, and and 60°. These angles are in a position to transfer momentum of light into the MSPs mode, leading to a reflectivity deep in the Otto ATR spectra (like Fig. 6). Note that one can clearly observe that only real modes (magnetostatic analog) can exist at the conditions, $a > b$.

Under an applied static magnetic field, on other hand, the numerical calculations should be required for this discussion shown in Fig. 14 [17]. Figure 14(a) shows a pure antiferromagnet (i.e. $f_1 = 1$); Fig. 14(b) shows $f_1 = 0.75$; Fig. 14(c) is $f_1 = 0.25$. For $f_1 = 1$ and $f_1 = 0.75$, one can observe that there are two magnetostatic modes and one is virtual mode at $\pm k_x$. As for $f_1 = 0.25$, there are all virtual modes at $\pm k_x$.

Finally, If $a = b$ ($f_1 = 0.5$), the dispersion relation of the antiferromagnetic superlattices (MnF_2) [4] is shown in Fig. 15. It shows the zero and non-zero applied static magnetic field, respectively. Fig. 15(a) shows the reciprocal dispersion relation; Fig. 15(b) shows

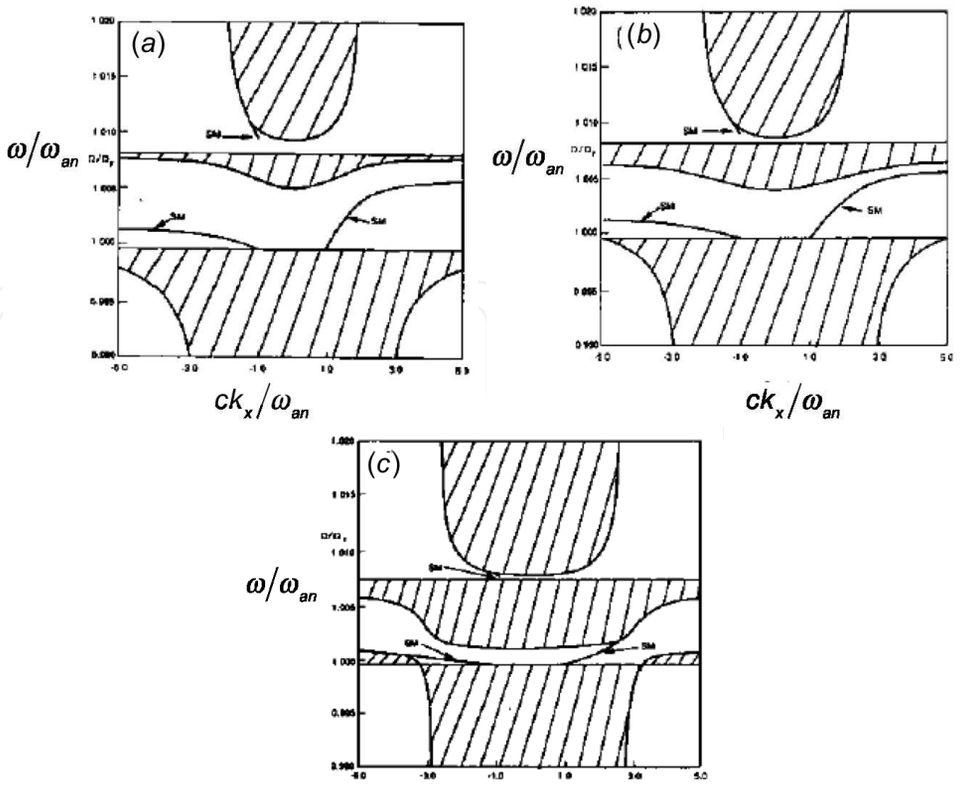


Figure 14. The dispersion relation at an applied static magnetic field. The solid curves represent the surface modes, and shaded regions are bulk modes. (a) a pure antiferromagnet (MnF_2) (b) antiferromagnetic superlattices, MnF_2/ZnF_2 ($f_1 = 0.75$). (c) antiferromagnetic superlattices, MnF_2/ZnF_2 ($f_1 = 0.25$). $\omega_{an} = 260\ GHz$. $H_0 = 200\ G$, $H_A = 7.85\ kG$, $H_E = 550\ kG$, $M_0 = 0.6\ kG$, $\varepsilon_{zz}^{(1)} = 5.5$, and $\varepsilon_{zz}^{(2)} = 8$. [3]

non-reciprocal dispersion relation. The MSPs modes only exist in a restricted region that bulk modes are not excited. Here, for consistence with reference [4], we recall the Eq. 35 and change the expression in Eq. 24 as following:

$$\omega_{an} = g\mu_0\gamma_0\sqrt{H_A\left(H_A + 2H_E\right)}\,. \tag{43}$$

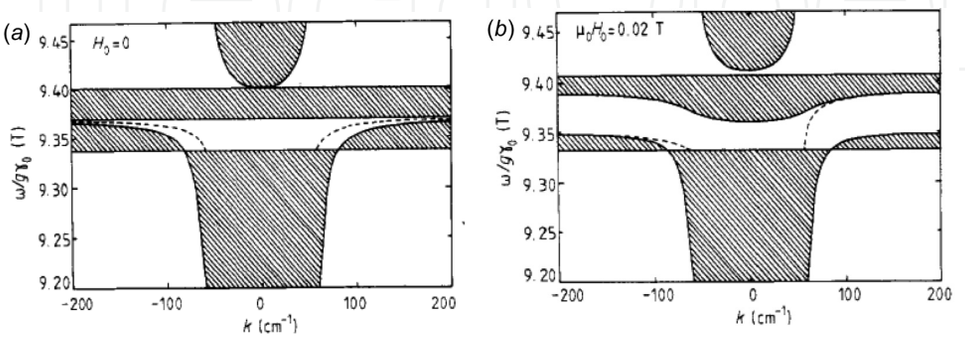


Figure 15. The antiferromagnetic (MnF_2)/nonmagnetic superlatticess. $a = b = 5 \times 10^{-4}\ cm$, $\mu_0 H_E = 55\ T$, $\mu_0 H_A = 0.787\ T$, $\mu_0 M_0 = 0.754\ T$, and $g = 2$. (a) $\mu_0 H_0 = 0$. (b) $\mu_0 H_0 = 0.02\ T$. The shaped region is the bulk polaritons; the dotted curve is the surface polaritons mode. [4]

6. Realization of MSPs by metamaterials

6.1. Introduction of metamaterials

In 1968, a Russian physicist V. G. Veselago theoretically calculated that a medium might bend light to the ”wrong” pathway whenever the medium could ”give” a negative refractive index [35]. In his theory, the negative refractive index medium (NRIM) is composed of both negative electric permittivity and negative magnetic permeability at the same time but unfortunately, Veselago never experimentaly demonstrated such an NRIM mainly because he could not find out a material with negative magnetic permeability. Three decades later, British physicist J.B. Pendry suggested that the two-dimensional metallic wires [12] and metallic split-ring resonators (SRRs) [11] yield to negative permittivity and negative permeability, respectively. These innovative electromagnetic responses were artificially created by a periodic array of sub-wavelength unit cells that afterwards, were termed as metamaterials and led to a variety of rare and even unprecedented electromagnetic properties such magnetic magnetism at terahertz region [33], inverse optical rules [e.g., inverse Snell’s law [22], inverse Doppler shift [30] and inverse Cerenkov radiation [28]] , superlensing effect [31], invisibility cloaking [7], and others.

In 2001, Shelby et al. integrated the metallic wires and metallic SRRs into a prism structure [see Fig. 16], and for the first time demonstrated the negative refractive index [22]. This result demonstrated that metamaterials were recognized to be an effective medium due to the sub-wavelength characteristics. Therefore, the magnetic metamaterials (like SRRs) can be expected to process the MSPs mode as same as that for the aforementioned magnetic superlattices. In fact, some groups have already theoretically predicated the surface mode of the ferromagnetic metals [1] and the metamaterials [26].

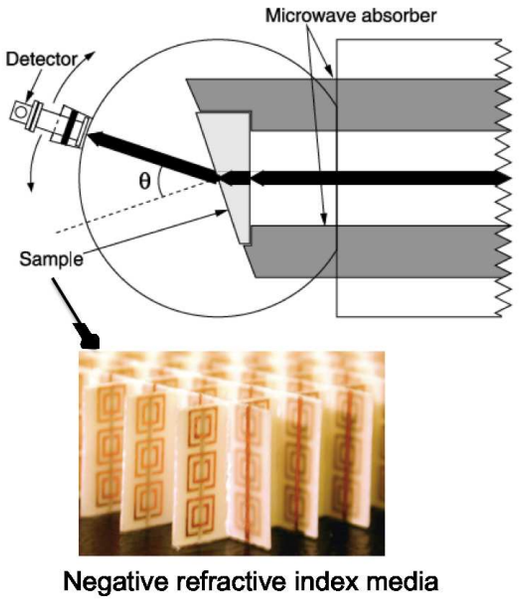


Figure 16. Experimental verification of the negative refractive index medium. The sample consisted of a periodic array of the metallic wires and the SRRs is so called a NRIM whose geometrical shape is a prism now. One can observe that the NRIM bends light into a "wrong" pathway, and Snell’s law verifies the negative refractive index. [22]

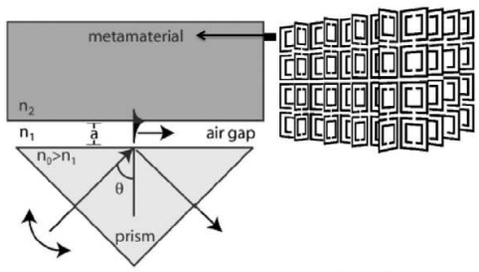


Figure 17. The Otto ATR configuration. The magnetic metamaterials is composed of a two-dimensional grid of the SRRs. "a" is gap between prism and metamaterials. [16]

6.2. Uniaxial magnetic metamaterials

Now, we quote an interesting work done by J. N. Gollub et at. who constructed a two-dimensional array of the SRRs into a physical three-dimensional bulk [16] shown in Fig. 17. Such the physical three-dimensional bulk metamaterials is considered as a semi-infinite medium due to the subwavelength SRR structure. According to their geometry, we regard the effective electric permittivity and magnetic permeability of the bulk as anisotropic and uniaxial, respectively. Therefore, it is straightforward to write

$$\begin{aligned} \overleftrightarrow{\varepsilon}_{eff}(\omega) &= \begin{pmatrix} \bar{\varepsilon}_{xx} & 0 & 0 \\ 0 & \bar{\varepsilon}_{yy} & 0 \\ 0 & 0 & \bar{\varepsilon}_{zz} \end{pmatrix}, \\ \overleftrightarrow{\bar{\mu}}_{eff}(\omega) &= \begin{pmatrix} \bar{\mu}_{xx} & 0 & 0 \\ 0 & \bar{\mu}_{xx} & 0 \\ 0 & 0 & \bar{\mu}_{zz} \end{pmatrix}. \end{aligned} \tag{44}$$

Also, the attenuation coefficients and dispersion equation of the surface mode of this bulk medium can be written by setting $\bar{\mu}_{xy} = 0$ and $\bar{\mu}_{xx} = \bar{\mu}_{yy}$ into Eqs. 8 and 13:

$$\begin{aligned} \alpha^{+} &= \sqrt{k_x^2 - \bar{\varepsilon}_{zz}\bar{\mu}_{xx}\frac{\omega^2}{c^2}}, \\ \alpha^{-} &= \sqrt{k_x^2 - \frac{\omega^2}{c^2}}, \end{aligned} \tag{45}$$

and

$$\frac{-\alpha^{+}}{\bar{\mu}_{xx}} = \alpha^{-}. \tag{46}$$

They are as same as those for a pure antiferromagnet without an applied static field [Eqs. 27 and 28]. The magnetic permeability of the bulk medium is calculated by means of the standard retrieval process [6, 34] shown in Fig. 18 [16]. There exists a $\bar{\mu}_{xx} < 0$ between 12 and 14 GHz in where the MSPs mode is expected. From Eq. 46, one knows that the momentum never be conserved without an optical coupler (diffraction gratings or prism). The experimental result of the Otto ATR spectra [16] is shown in Fig. 19 , where the dash curve is numerical calculation and the solid curve is experimental measurement. The experimental result is in a good agreement with numerical calculation, and demonstrated successfully that the MSPs mode is excited occurring at reflectivity deep (12.2 GHz).

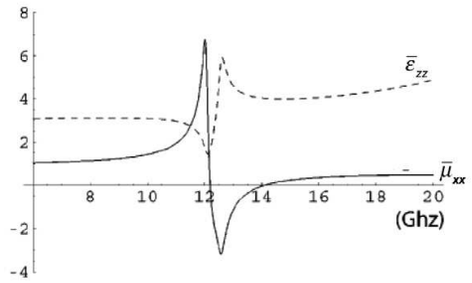


Figure 18. The effective permittivity and permeability of the bulk metamaterials. $\bar{\mu}_{xx} < 0$ for 12 and 14 GHz. [16]

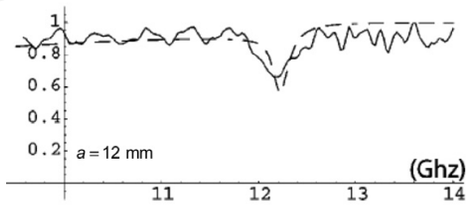


Figure 19. The experimental results of the ATR spectra, and $a = 12\ mm$. The dash curve is numerical calculation, and the solid curve is experimental measurement. [16]

6.3. Biaxial magnetic metamaterials

Here, we shortly re-describe what we just talked about the conditions for an excitation of the MSPs at magnetostatic limit. First, for a pure uniaxial ferromagnet, the MSPs can be excited at the condition, $\mu_{xx} \pm \mu_{xy} = -1$ [Eq. 17] with an applied static magnetic field. Note that the surface mode might exist whether or not the μ_v in Fig. 3 is positive or negative. Second, for a pure antiferromagnet without an applied static field, the condition is $\mu_{xx} = -1$ at magnetostatic limit, which is also for uniaxial magnetic metamaterials. Third, for a ferromagnetic superlattices, the condition is not considered in this chapter, but we present a special numerical result shown in Fig. 11. Fourth, for an antiferromagnetic superlattices, the necessary condition is $\bar{\mu}_{xx} < 0$. It collocates with $\bar{\mu}_{yy} < 0$ being a real mode and $\bar{\mu}_{xy} > 0$ being a virtual mode, respectively.

Now, we would like to introduce our previous work [37] that considered a situation as same as the antiferromagnetic superlattices. In a word, the magnetic metamaterials have an effect biaxial tensors are given by

$$\begin{aligned} \overleftrightarrow{\varepsilon}_{eff}(\omega) &= \begin{pmatrix} \bar{\varepsilon}_{xx} & 0 & 0 \\ 0 & \bar{\varepsilon}_{yy} & 0 \\ 0 & 0 & \bar{\varepsilon}_{zz} \end{pmatrix}, \\ \overleftrightarrow{\mu}_{eff}(\omega) &= \begin{pmatrix} \bar{\mu}_{xx} & 0 & 0 \\ 0 & \bar{\mu}_{yy} & 0 \\ 0 & 0 & \bar{\mu}_{zz} \end{pmatrix}. \end{aligned} \tag{47}$$

The proposal structure of our work [shown in Fig. 20] is a periodic array of the sandwich unit cells. Fig. 20(b) shows there are three layers in a sandwich unit cell that includes two SRRs and one spacer (Roger RT5800). The dimension of the unit cell is $6 \times 6\ mm^2$ and thickness is $2\ mm$, which is smaller than our operating wavelength (23 mm or 13.22 GHz). Therefore, it is safe to consider a sandwich unit cell as an effective medium. Its effective electric permittivity

and magnetic permeability are retrieved shown in Fig. 21. At 13.22 GHz, we have

$$\bar{\mu}_{xx} = -4.20,\ \bar{\mu}_{yy} = -0.252,\ \bar{\varepsilon}_{zz} = 3.46. \tag{48}$$

Therefore, our design only possesses the real mode. Using COMSOL Multiphysics finite element based electromagnetic solver [2], we simulate the field distribution of the MSPs mode shown in Fig. 22 where one can clearly see the exponential decay of the MSPs propagating at the interface. By substituting Eq. 48 into Eq. 40, the wavelength of the MSPs mode can be evaluated as 3.947 mm that is in a good agreement with the simulation result (not shown). Note that such a biaxial magnetic metamaterials depends on designed geometry to determine the resonance frequency of the MSPs mode, instead of inherent magnetism.

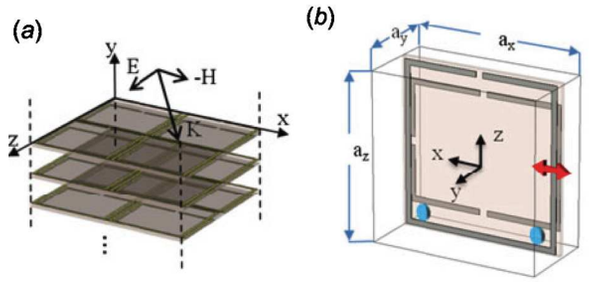


Figure 20. The sandwich unit cell of the biaxial magnetic metamaterials. $a_x = a_y = 6\ mm, a_z = 2\ mm$. [37]

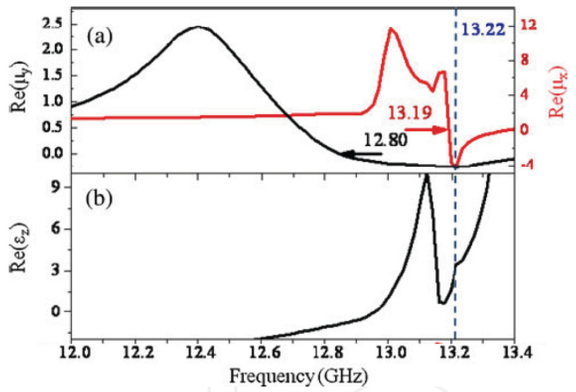


Figure 21. The retrieval result of the biaxial magnetic metamaterials. (a) Red curve is $\bar{\mu}_{xx}$; black curve is. (b) Black curve is $\bar{\varepsilon}_{zz}$. At 13.22 GHz, we have $\bar{\mu}_{xx} = -4.2, and \bar{\mu}_{yy} = -0.252, \bar{\varepsilon}_{zz} = 3.46$. [37]

6.4. One-dimensional magnetic photonic crystal

In last two sections, the samples are not composed of magnetic materials, and so there need not be an applied static magnetic field. Now, we basically introduce that a magnetic metamaterials is composed of YIG rods [29] shown in Fig. 23(a). The structure is like a one-dimensional photonic crystal (PC), and arranged periodically in a square lattice embedded within the air. The lattice constant is $a = 8\ mm$ and the radius of the YIG rod is $r = 2\ mm$ where axis of the rods is at $\widehat{z}$ axis. Again, an applied magnetic static field is along the easy axis $\widehat{z}$. The operating frequency is 5 GHz (i.e. wavelength = 60 mm) that is enough

[2] http://www.comsol.com/

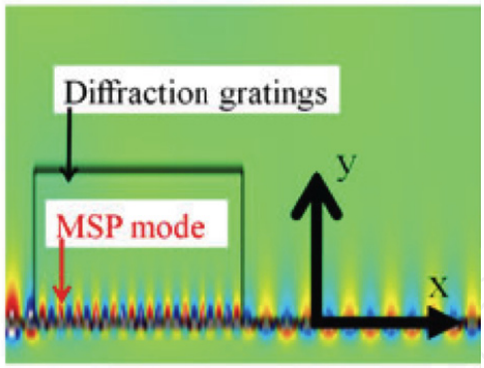


Figure 22. The field distribution of the MSPs mode for a biaxial magnetic metamaterials at 13.22 GHz. [37]

lager to be regarded this structure as an effective medium. For the reflectivity simulation, the magnetic permeability of the YIG needs a damping factor that can be modified from Eq. 14:

$$\omega_0 \rightarrow \omega_0 + i\beta\omega \tag{49}$$

The retrieved effective permittivity and permeability, and band diagram of the bulk polaritons are plotted in Figs. 23(c) and 23(b), respectively. Note that the condition of the magnetostatic mode is as same as that for a pure ferromagnet [i.e. see Eq. 17]. In a word, the condition is $\mu_{eff} = -1$ [see in Fig. 23(c)]. In this work, Liu et al. planed to apply a static magnetic field upon the PC, which yields to the modeling of the reflectivity as shown in Fig. 23(a). One can observe the reflectivity has "own" direction at the resonance frequency of the

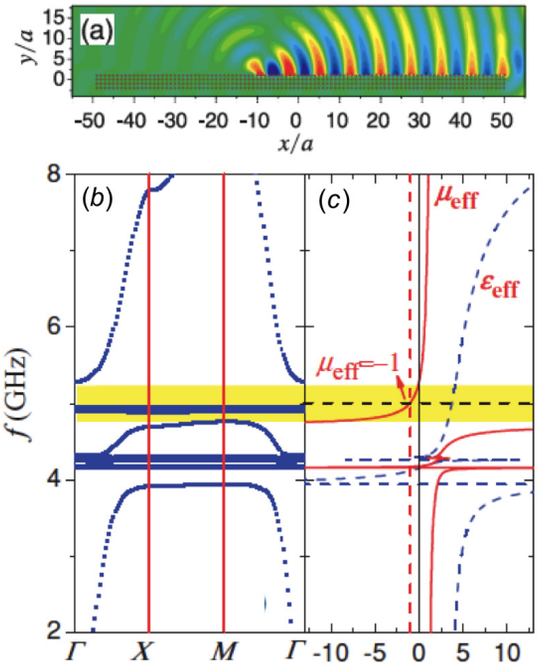


Figure 23. (a) The line source is transverse magnetic wave with the electric field polarized along the rod, and is placed near the surface of the magnetic metamaterials ($\frac{y}{a} = 1$; $\frac{x}{a} = -10$) (b) The photonic band diagram of the magnetic metamaterials with $H_0 = 900\ Oe$. The yellow region is photonic band gap. (c) The retrivevd effective constitutive parameters. The blue dashed curve is ε_{eff} and red solid curve is μ_{eff}. Note that $\mu_{eff} = 1$ at 5 GHz. [29]

MSPs. The main mechanism is non-reciprocal dispersion relation of the MSPs because the left-propagating direction of the MSPs is forbidden.

7. Conclusions

In this study, we review a few important papers that help one to understand the conditions about the existence of the magnetic surface polaritons (MSPs) modes. Note that ferromagnetic resonance frequency is typically in the microwave frequency region, and antiferromagnetic resonance frequency in the far infrared. However, Metamaterials resonance frequency can be artificially determined.

The MSPs mode can further be considered as two kinds of modes, real mode (magnetostatic analog) and virtual mode. First, for real mode, we basically summarize those aforementioned conditions. (a) For a pure uniaxial ferromagnet with $\overleftrightarrow{\varepsilon} = 1$, at an external static magnetic field (H_0), the condition is $\mu_0 \left[1 + \omega_m/(\omega_0 - \omega)\right] = -1$ where ω_{msp} is locating within the region, $\mu_V < 1$. In addition, the dispersion relation of the MSPs mode is non-reciprocal. On the other hand, without H_0, the condition is $\mu_0 \left[1 - \omega_m/\omega\right] = -1$ and magnetostatic analog starts at $k_x = 0$ with non-reciprocal dispersion relation. (b) For a pure uniaxial anti-ferromagnet, without H_0, the condition is $\mu_{xx} = -1$ where ω_{msp} is living within the region, $\mu_V < 1$. The dispersion relation of the MSPs is reciprocal. On other hand, with H_0, numerical calculation shows there is a possibility to have a magnetostatic analog with non-reciprocal dispersion relation. (c) For a ferromagnetic superlattices, with H_0, there is a magnetostatic analogs for $a/b > 0.5$. The dispersion relation of the MSPs is non-reciprocal. (d) For an anti-ferromagnetic superlattices, without H_0, the condition is $\bar{\mu}_{xx} = -1$ and $\bar{\mu}_{xx}\bar{\mu}_{yy} = 1$. The dispersion relation of the MSPs mode is reciprocal for $a > b$. On other hand, with H_0, numerical calculation shows that the magnetostatic analog can exist for $a > b$.

Second, for the virtual modes, the numerical calculation is necessary, and it is not easy to give a exact condition. However, for magnetic superlattices, if the ratio of "a" to "b" is less than 0.5, then the virtual modes should exist. Finally, let us comment the conditions for magnetic metamaterials. The magnetic metamaterials are ability to design their constitutive parameters by means of a specific the geometry of the sub-wavelength unit cell. Theoretically, one can well control the real modes or virtual modes, yielding to the versatile devices such as optical bistability [9, 10, 13], second harmonic generation [19]. Although over the past researches have less attention to the MSPs modes due to the experimental difficulty compared to electric SPPs, we expect the MSPs mode will get more attention by means of the magnetic metamaterials in the future.

Acknowledgments

The authors would like to gratefully acknowledge the financial support from the National Science Council (98-2112-M-007-002MY3, 99-2923-M-007-003-MY2, 99-ET-E-007-002-ET, 100-ET-E-007-002-ET, 100-2120-M-002-008, 100-2120-M010-001).

Author details

Yu-Hang Yang and Ta-Jen Yen
Department of Materials Science and Engineering, National Tsing Hua University, Hsinchu, Taiwan

8. References

[1] A. Hartstei, E. Burstein, A. M. R. B. & Wallis, R. F. [1973]. Surface polaritons on semi-infinite gyromagnetic media, *Journal of Physics C-Solid State Physics* 6(7): 1266–1276.
[2] Almeida, N. S. & Mills, D. L. [1988]. Effective-medium theory of long-wavelength spin-waves in magnetic superlattices, *Physical Review B* 38(10): 6698–6710.
[3] Almeida, N. S. & Tilley, D. R. [1990]. Surface-polaritons on antiferromagnetic superlattices, *Solid State Communications* 73(1): 23–27.
[4] Barnas, J. [1990]. Spin-waves in superlattices .3. magnetic polaritons in the voigt configuration, *Journal of Physics-Condensed Matter* 2(34): 7173–7180.
[5] Camley, R. E. & Mills, D. L. [1982]. Surface polaritons on uniaxial antiferromagnets, *Physical Review B* 26(3).
[6] D. R. Smith, S. Schultz, P. M. & Soukoulis, C. M. [2002]. Determination of effective permittivity and permeability of metamaterials from reflection and transmission coefficients., *Phys. Rev. B* 65: 195104.
[7] D. Schurig, J. J. Mock, B. J. J. S. A. C. J. B. P. A. F. S. & Smith, D. R. [2006]. Metamaterial electromagnetic cloak at microwave frequencies, *Science* 314(5801): 977–980.
[8] Damon, R. W. & Eshbach, J. R. [1961]. Magnetostatic modes of a ferromagnet slab, *Journal of Physics and Chemistry of Solids* 19(3-4): 308–320.
[9] G. D. Xu, T. Pan, T. C. Z. & Sun, J. [2008]. Optical bistability with surface polaritons in layered structures containing left-handed metallic magnetic composites, *Applied Physics B-Lasers and Optics* 93(2-3): 551–557.
[10] I. L. Lyubchanskii, N. N. Dadoenkova, A. E. Z. Y. P. L. & Rasing, T. [2008]. Optical bistability in one-dimensional magnetic photonic crystal with two defect layers, *Journal of Applied Physics* 103(7).
[11] J. B. Pendry, A. J. Holden, D. J. R. & Stewart, W. J. [1999]. Magnetism from conductors and enhanced nonlinear phenomena, *Ieee Transactions on Microwave Theory and Techniques* 47(11): 2075–2084.
[12] J. B. Pendry, A. J. Holden, W. J. S. & Youngs, I. [1996]. Extremely low frequency plasmons in metallic mesostructures, *Physical Review Letters* 76(25): 4773–4776.
[13] J. Bai, S. F. Fu, S. Z. & Wang, X. Z. [2011]. Reflective optical bi-stability of antiferromagnetic films, *European Physical Journal B* 83(3): 343–348.
[14] J. Matsuura, M. F. & Tada, O. [1983]. Atr mode of surface magnon polaritons on yig, *Solid State Communications* 45(2).
[15] J. N. Anker, W. P. Hall, O. L. N. C. S. J. Z. & Duyne, R. P. V. [2008]. Biosensing with plasmonic nanosensors, *Nature Materials* 7(6): 442–453.
[16] J. N. Gollub, D. R. Smith, D. C. V. T. P. & Mock, J. J. [2005]. Experimental characterization of magnetic surface plasmons on metamaterials with negative permeability, *Physical Review B* 71(19).
[17] M. C. Oliveros, N. S. Almeida, D. R. T. J. T. & Camley, R. E. [1992]. Magnetostatic modes and polaritons in antiferromagnetic nonmagnetic superlattices, *Journal of Physics-Condensed Matter* 4(44): 8497–8510.
[18] M. R. F. Jensen, T. J. Parker, K. A. & Tilley, D. R. [1995]. Experimental-observation of magnetic surface-polaritons in fef2 by attenuated total-reflection, *Physical Review Letters* 75(20): 3756–3759.
[19] M. W. Klein, C. Enkrich, M. W. & Linden, S. [2006]. Second-harmonic generation from magnetic metamaterials, *Science* 313(5786): 502–504.

[20] Mills, D. L. & Burstein, E. [1974]. Polaritons - electromagnetic modes of media, *Reports on Progress in Physics* 37(7): 817–926.
[21] Pincus, P. [1962]. Propagation effects on ferromagnetic resonance in dielectric slabs, *Journal of Applied Physics* 33(2): 553.
[22] R. A. Shelby, D. R. S. & Schultz, S. [2001]. Experimental verification of a negative index of refraction, *Science* 292: 77.
[23] R. E. Camley, M. G. C. & Tilley, D. R. [1992]. Surface-polaritons in antiferromagnetic superlattices with ordering perpendicular to the surface, *Solid State Communications* 81(7): 571–574.
[24] Raether, H. [1988]. *Surface plasmons on smooth and rough surfaces and on gratings*, Springer-Verlag.
[25] Raj, N. & Tilley, D. R. [1987]. Polariton and effective-medium theory of magnetic superlattices, *Physical Review B* 36(13): 7003–7007.
[26] Ruppin, R. [2000]. Surface polaritons of a left-handed medium, *Physics Letters A* 277(1): 61–64.
[27] S. Lal, S. L. & Halas, N. J. [2007]. Nano-optics from sensing to waveguiding, *Nature Photonics* 1(11): 641–648.
[28] S. Xi, H. S. Chen, T. J. L. X. R. J. T. H. B. I. W. J. A. K. & Chen, M. [n.d.]. Experimental verification of reversed cherenkov radiation in left-handed metamaterial, *Physical Review Letters* 103(19).
[29] S. Y. Liu, W. L. Lu, Z. F. L. & Chui, S. T. [2011]. Molding reflection from metamaterials based on magnetic surface plasmons, *Physical Review B* 84(4).
[30] Seddon, N. & Bearpark, T. [2003]. Observation of the inverse doppler effect, *Science* 302(5650): 1537–1540.
[31] Smolyaninov, II, Y. J. H. & Davis, C. C. [2007]. Magnifying superlens in the visible frequency range, *Science* 315(5819): 1699–1701.
[32] Stamps, R. L. & Camley, R. E. [1989]. Greens-functions for antiferromagnetic polaritons .2. scattering from rough surfaces, *Physical Review B* 40(1): 609–621.
[33] T. J. Yen, W. J. Padilla, N. F. D. C. V. D. R. S. J. B. P. D. N. B. & Zhang, X. [2004]. Terahertz magnetic response from artificial materials, *Science* 303(5663): 1494–1496.
[34] T. M. G. Xudong Chen, B.-I. W., Pacheco, J. J. & Kong, J. A. [2004]. Robust method to retrieve the constitutive effective parameters of metamaterials, *PHYSICAL REVIEW E* 70: 016608.
[35] Veselago, V. G. [1968]. Electrodynamics of substances with simultaneously negative values of sigma and mu, *Soviet Physics Uspekhi-Ussr* 10(4): 509.
[36] Wang, X. Z. & Tilley, D. R. [1995]. Retarded modes of a lateral antiferromagnetic nonmagnetic superlattice, *Physical Review B* 52(18): 13353–13357.
[37] Y.H. Yang, I. W., U. H. L. & Yen, T. [2012]. Magnetic surface polariton in a planar biaxial metamaterial with dual negative magnetic permeabilities, *Plasmonics* 7(1): 87–92.